

EFFECTIVE DYE REMOVAL FROM WASTE WATER USING A NOVEL LOW-COST NaOH-MODIFIED FLY ASH

XIAOMING GAO*, YUAN DAI, YU ZHANG, XIANG ZHAI, AND FENG FU

Department of Chemistry and Chemical Engineering, Shaanxi Key Laboratory of Chemical Reaction Engineering, Yan'an University, Yan'an, Shaanxi 716000, China

Abstract—Dyes are toxic and considered to be extremely hazardous to natural environments. Hence, adsorbents to remove dyes from contaminated water are needed. To develop adsorbents with a high adsorption capacity for different dyes, easy separation, and low cost, a novel dye adsorbent was prepared by activating fly ash with NaOH. The adsorbent morphology, structure, and specific surface area were characterized using scanning electron microscopy, X-ray powder diffraction, and surface area measurements using N₂ adsorption-desorption. The adsorption abilities of the synthesized adsorbents were examined based on methylene blue and acid fuchsin adsorption from water. The capabilities of the adsorbents as a function of adsorbent use, dye type, dye concentration, time, and pH were investigated and compared. The results for methylene blue and acid fuchsin adsorption were modeled using pseudo-second order kinetics and the Langmuir adsorption isotherm, respectively. These modified adsorbents synthesized from fly ash may provide a promising solution to purify dye-contaminated waste water with the advantages of high efficiency and low cost.

Key Words—Acid Fuchsin, Adsorption, Dye Adsorption, Methylene Blue, NaOH-Modified Fly Ash, Wastewater Treatment.

INTRODUCTION

Dyes are considered to be extremely hazardous because of the toxicity to and long-lasting effects (do not degrade readily in nature) on plants, aquatic organisms, animals, and humans. The present study tested the hypothesis that these organic pollutants can be removed effectively from waste water by such methods as coagulation (Zhang *et al.*, 2013a), flocculation (Zhao *et al.*, 2009), membrane separation (Tang *et al.*, 2014), oxidation, ozonation (Ji *et al.*, 2015), solvent extraction (Liao *et al.*, 2014), electro-coagulation (Liu *et al.*, 2013), and adsorption (Wang *et al.*, 2014a, 2014b), all of which have been developed to remove pollutants from waste water. Among these methods, adsorption is effective and promising (Hassan *et al.*, 2015; Wang *et al.*, 2011; Anirudhan *et al.*, 2010; Torrellas *et al.*, 2015). Considerable attention has been devoted to developing high-efficiency adsorbents, such as activated carbons (Sevilla *et al.*, 2014; Baur *et al.*, 2015; Choi *et al.*, 2009), clays (Frydrych *et al.*, 2011; Zhang *et al.*, 2013b; Gupta *et al.*, 2012, 2014; Wang *et al.*, 2013; Akar *et al.*, 2013; Lee *et al.*, 2015; Akkaya, 2013; Kim *et al.*, 2015; Fu *et al.*, 2011), metal complexes (Zheng *et al.*, 2014; Sun *et al.*, 2012; Yang *et al.*, 2015; Upadhyay *et al.*, 2014), porous polyacrylamide (Idris *et al.*, 2015), macroporous polydivinylbenzene/polyacryldiethylenetriamine

(PDVB/PADETA) (Wang *et al.*, 2014a), MOFs (Petit *et al.*, 2011; Cavka *et al.*, 2014; Liu *et al.*, 2012), and so on. However, most of these adsorbents still suffer from high cost and limited regeneration ability, which hinders applications in industrial waste water purification.

Interestingly, highly porous adsorbents with a high adsorption capacity for aqueous dyes have been prepared from low-cost materials, *i.e.*, fly ash. Fly ash, a solid waste mainly generated from power plants, has received wide attention due to unique properties that include low cost, porous structure, light weight, corrosion resistance, good fluidity, easy dispersion, thermal stability, and low toxicity (Ahmed *et al.*, 2014; Shi *et al.*, 2011; Pizarro *et al.*, 2015). These features may enable fly ash to be used for dye removal from waste water. Pristine fly ash, however, consists of glass beads with a small particle size, small surface area, and inert chemical properties. The purpose of this work was to activate fly ash by treatment with NaOH to yield a novel fly ash-based dye adsorbent, which would take full advantage of this waste material. The adsorption capability was examined in terms of dye concentration, adsorbent usage, pH, and contact time. The adsorption mechanism and the adsorption/desorption behavior of NaOH-modified fly ash were analyzed using adsorption kinetics and adsorption isotherms.

MATERIALS AND METHODS

Fly ash was obtained from the Shaanxi Yulin electric power plant. The fly ash was washed several times with distilled water and ethanol and then dried at 60°C in air for 8 h. The methylene blue and acid fuchsin dyes were

* E-mail address of corresponding author:

dawn1026@163.com

DOI: 10.1346/CCMN.2016.064028

analytical reagent grade and were obtained from Sinopharm Chemical Reagent Co., Ltd., China.

PREPARATION AND CHARACTERIZATION OF NaOH-MODIFIED FLY ASH

Preparation

In a typical preparation process, 0.5 g of the NaOH-modified fly ash was added to 20 mL of NaOH solution with concentrations of 2, 4, 6, and 8 mol/L. The resulting mixtures were vigorously stirred for 30 min using a magnetic stirrer at 30°C and then dried at 105°C in a drying oven. The prepared samples were named S1 (fly ash modified with 2 mol/L NaOH), S2 (fly ash modified with 4 mol/L NaOH), S3 (fly ash modified with 6 mol/L NaOH), and S4 (fly ash modified with 8 mol/L NaOH), respectively.

Characterization

The morphologies and microstructures of the NaOH-modified fly ash were analyzed using a Hitachi TM-3000 scanning electron microscope (Hitachi Ltd., Tokyo, Japan). The phase and composition of NaOH-modified fly ash samples were identified using X-ray diffraction with monochromatic CuK α radiation generated at 40 kV and 100 mA and scanned from 10 to 80°2 θ using a Shimadzu XRD-7000 X-ray diffractometer (Shimadzu Corporation, Kyoto, Japan). The specific surface areas and porosities of the NaOH-modified fly ash samples were measured at liquid N₂ temperature using a Micromeritics ASAP2020 (Micromeritics, Norcross, Georgia, USA).

Adsorption experiments

Methylene blue (MB) (a) and acid fuchsin (AF) (b) were used in the adsorption experiments (Figure 1). Typically, adsorption experiments were carried out by adding 50 mL of dye solution with the desired initial concentrations and pH into a series of 100 mL conical flasks that contained certain amounts of the NaOH-modified fly ash samples. To attain equilibrium, the conical flasks were maintained at an agitation speed of 140 rpm for 3–12 h. Subsequently, the adsorbent was separated from the dye solution by centrifugation. The residual concentration of dye in solution was determined

using UV-VIS spectroscopy to measure the absorbance changes at the maximum absorbance wavelength. The effect of pH on dye removal was analyzed in the 2 to 10 pH range. The solution pH was adjusted using acetic acid buffer.

The dye removal efficiency and the equilibrium amount (q_e , mg/g) adsorbed were calculated using the following equation:

$$\text{Removal Efficiency} = \frac{(c_0 - c_e)}{c_0} \times 100\% \quad (1)$$

$$q_e = \frac{V(c_0 - c_e)}{m} \quad (2)$$

where q_e (mg/g) was the equilibrium dye adsorption capacity per unit mass of adsorbent at equilibrium; c_0 (mg/L) and c_e (mg/L) were the initial and equilibrium dye concentrations, respectively; V (mL) was the total solution volume; and m (g) was the adsorbent mass. All of the experiments were run in duplicate and the deviations between duplicates were within 5%.

RESULTS AND DISCUSSION

Characterization

The phase, crystallinity, and purity of the NaOH-modified fly ash samples were examined using X-ray diffraction (XRD) and typical diffraction patterns are presented in Figure 2. With increased NaOH solution concentrations, the characteristic mullite diffraction peak gradually weakened, whereas the characteristic quartz diffraction peaks remained basically unchanged. This indicates that higher NaOH solution concentrations significantly destroyed the mullite mineral phase. In the hydrothermal modification, quartz in the fly ash resisted NaOH erosion, but reacted with the weakly crystalline mullite. Especially, under the auto-generated pressure and high temperature, NaOH reacted with soluble SiO₂ in the mullite (3Al₂O₃·2SiO₂ or 2Al₂O₃·SiO₂) to generate Na₂SiO₃, which acted as a material binder with a good viscosity and strength. Thus, the higher the NaOH solution concentration used, the more active components were dissolved. The fly ash with higher viscosity yielded more granular reaction products.

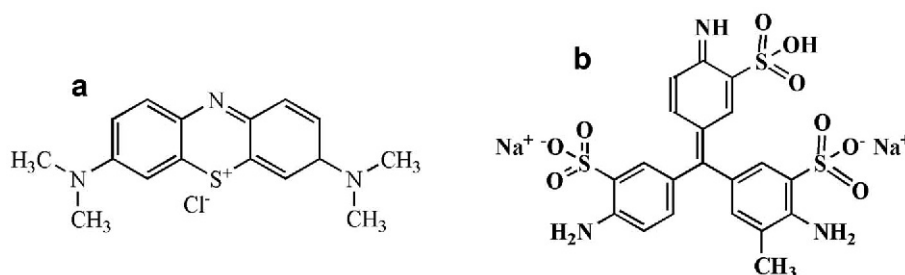


Figure 1. The molecular structures of (a) methylene blue (MB) and (b) acid fuchsin (AF).

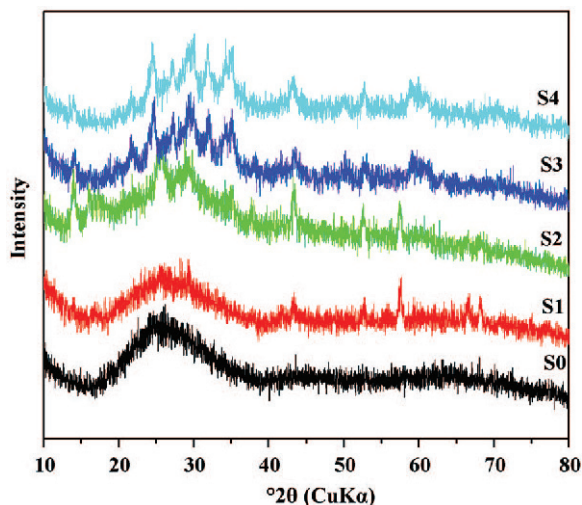


Figure 2. XRD patterns of samples: S0 = unmodified fly ash, S1 = fly ash modified with 2 mol/L NaOH, S2 = fly ash modified with 4 mol/L NaOH, S3 = fly ash modified with 6 mol/L NaOH, and S4 = fly ash modified with 8 mol/L NaOH.

Experimental measurements of fly ash morphology (Figure 3a) revealed that the mineral phase of the fly ash was mainly glass beads. The untreated fly ash micro-morphology was regular spherical particles with smooth and compact surfaces. After modification with NaOH solution, as shown in Figures 3b–f, the surface roughness of the fly ash was significantly increased and part of the glass bead was dissolved to form irregular shapes. With increased NaOH solution concentrations, the roughness and deformation of the fly ash glass beads increased. In particular, when the NaOH solution concentration was 4 mol/L, the spherical fly ash structure was difficult to identify. The alkaline NaOH remarkably destroyed the polymeric silicate glass structure of the fly ash, dissolved soluble SiO_2 , and the polymeric silicate was decomposed into oligomeric silicates. Hence, the NaOH solution reacts with silica in the fly ash to generate zeolites (Koukouzas *et al.*, 2010).

Experimental measurements of the specific surface area of the unmodified fly ash (S0) and the modified fly ash S1, S2, S3, and S4 (Table 1) revealed a significant increase in the specific surface area of the modified fly ash. When NaOH solution concentrations were less than 6 mol/L, the specific surface area increased significantly with increased NaOH solution concentrations. The lower surface area of the unmodified fly ash was due to the

regular spherical particle shape with smooth and compact surfaces. When modified with NaOH solution, the fly ash glass beads were partially dissolved to form irregular shapes with significantly rougher surfaces. As NaOH solution concentrations were increased above 6 mol/L, however, the irregular fly ash was further destroyed to form fine particles with a decreased specific surface area. Thus, the NaOH concentration was a very important factor in the specific surface area of the modified fly ash. Experimental N_2 adsorption/desorption measurements yielded N_2 adsorption isotherms and the pore size of sample S4 (Figure 4). According to the IUPAC classification (Sing *et al.*, 1985), N_2 adsorption isotherms of the modified fly ash were categorized as type IV. The isotherm curves rose rapidly in the low pressure area, were smooth and flat in the medium pressure area, and had an apparent hysteresis loop in the high pressure area. In particular, the adsorption isotherm became obviously flat in the 0.3 to 0.8 p/p_0 range, which is characteristic of mesoporous structures. The pore-size distribution of sample S4 spanned approximately 2–10 nm (Figure 4 inset) and indicate this sample has relatively uniform mesopores.

Adsorption properties of NaOH-modified fly ash

Methylene blue (MB) and acid fuchsin (AF) were used to study the adsorption properties of the NaOH-modified fly ash. Dye chemical structures and the solution adsorption spectra were illustrated and measured (Figure 5). The NaOH-modified fly ash could be easily dispersed in dye solutions to form dark-brown suspensions. After 1 h, the solution color significantly faded and dye solution adsorption spectra clearly disappeared, which indicates that the NaOH-modified fly ash had an excellent adsorption capacity for the dye.

Effects of NaOH concentration relative to fly ash

Experiments to determine the effects of NaOH solution concentrations on the decolorization of dyes were conducted. According to the experimental results, the NaOH-modified fly ash adsorbed the MB and AF dyes (Figure 6). Experimental measurements revealed that the decolorization rates of the unmodified fly ash for MB and AF dyes were relatively low, with maximum decolorization rates of 7.66 and 20.93%, respectively. However, adding NaOH-modified fly ash to the dye solutions significantly increased the decolorization. When the concentration of NaOH solution was 2 mol/L, the decolorization of MB and AF within

Table 1. The specific surface area (m^2/g) of the fly ash.

Samples	S0	S1	S2	S3	S4
$S_{(\text{BET})}$	3.32	67.25	85.33	130.98	82.34
$S_{(\text{Langmuir})}$	4.52	88.39	113.30	176.16	109.19

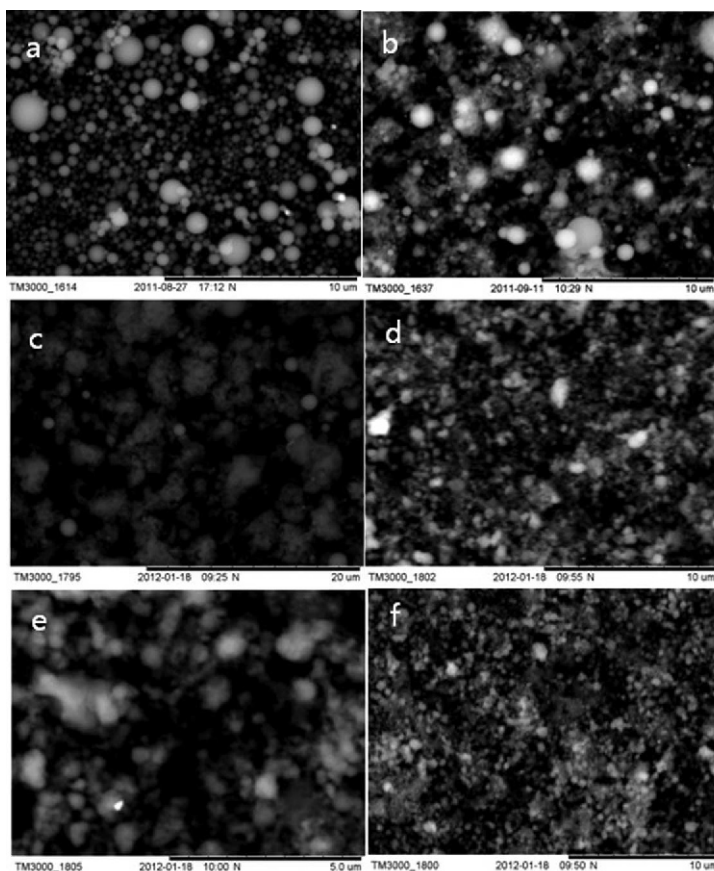


Figure 3. Sample SEM micrographs: (a) unmodified fly ash, (b) fly ash modified with 2 mol/L NaOH, (c) fly ash modified with 4 mol/L NaOH, (d) and (e) fly ash modified with 6 mol/L NaOH at different magnifications, and (f) fly ash modified with 8 mol/L NaOH.

10 min was 87.23 and 83.69%, respectively. While the NaOH solution concentration was 6 mol/L, the MB and AF decolorization rates reached maximum values of 96.02 and 91.96%, respectively. When NaOH solution

concentrations higher than 6 mol/L were used, no significant influence of NaOH solution concentration on dye adsorption was evident. The surface of the NaOH-modified fly ash was rough and porous, which

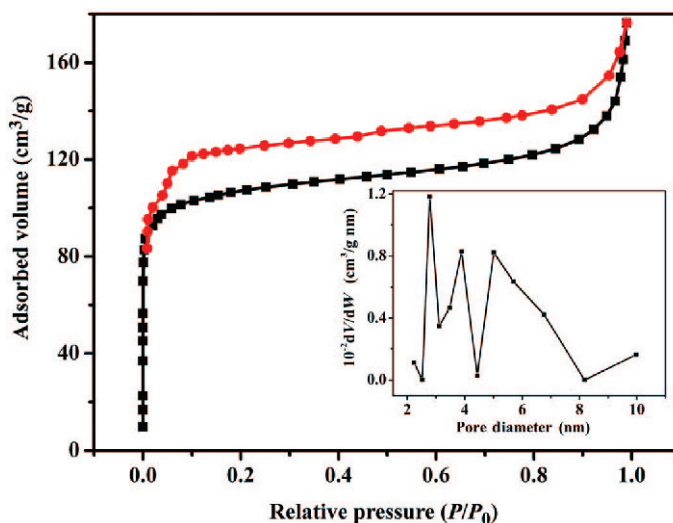


Figure 4. Adsorption/desorption isotherms and (inset) Barret-Joyner-Halenda (BJH) pore size distribution plots of sample S4.

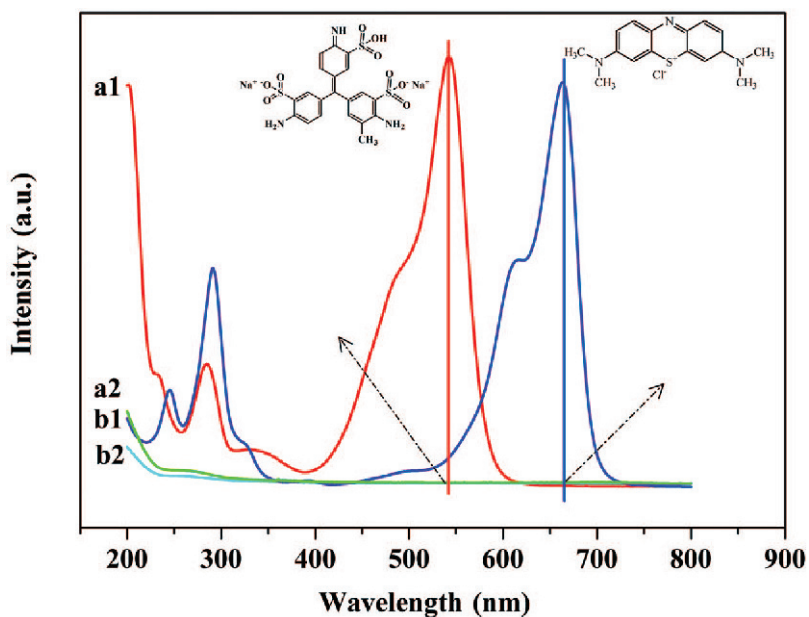


Figure 5. Adsorption spectra of (a1) AF and (b1) MB solutions before adsorption and adsorption spectra of (a2) AF and (b2) MB solutions after adsorption. The structural formulas of AF and MB and the effect of adsorption to NaOH-modified fly ash. Experimental conditions: pH = 2, 30°C, 50 mL of a 30 mg/L initial MB or AF solution concentration.

resulted in an increased specific surface area. On the other hand, NaOH could dissolve SiO_2 and Al_2O_3 in the fly ash to generate a secondary hydrate and the Si–O and Al–O bonds in the fly ash were broken in the hydrothermal environment. Thereby, dye adsorption by the modified fly ash was greatly improved. When NaOH solution concentrations were too high, the fly ash was further destroyed, formed fine particles, and the adsorption capacity was decreased.

Effects of NaOH-modified fly ash on dye solution decolorization

The effects of using NaOH-modified fly ash for decolorizing dye solutions were carried out using 0.05–0.15 g of adsorbent in 50 mL of solution containing 30 mg/L of MB or AF. The removal of MB and AF by 0.05–0.15g of NaOH-modified fly ash increased significantly with increased adsorbent weight (Figure 7). No significant increase of decolorization rate was found even when 0.10 to 0.15 g of adsorbent was used.

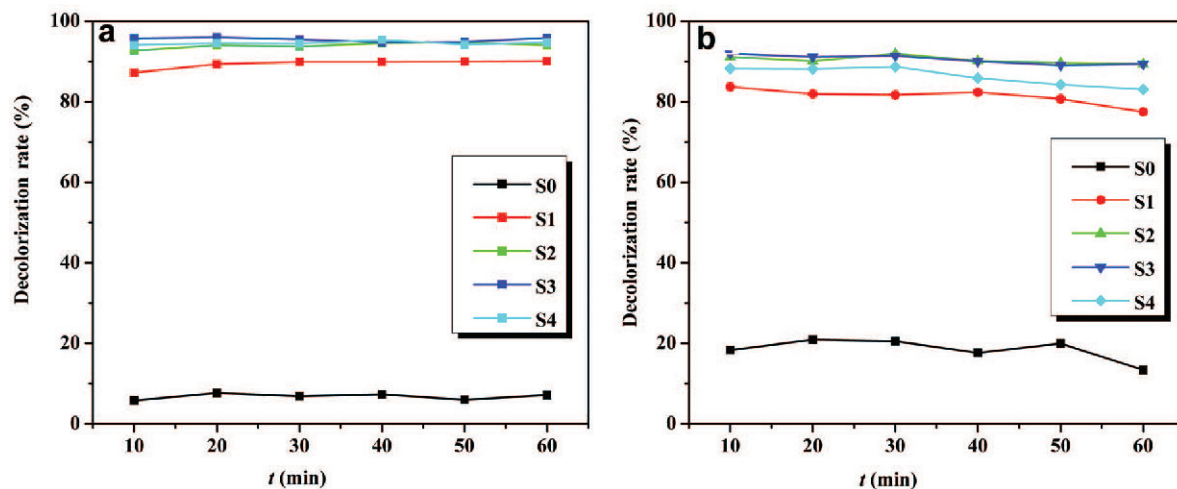


Figure 6. The effect of NaOH solution concentrations used to prepare NaOH-modified fly ash on the decolorization rate of (a) MB and (b) AF on fly ash: Sample designations are the same as in Figure 1. Experiment conditions: pH = 2, 30°C, 50 mL volume, and 30 mg/L initial MB or AF concentration.

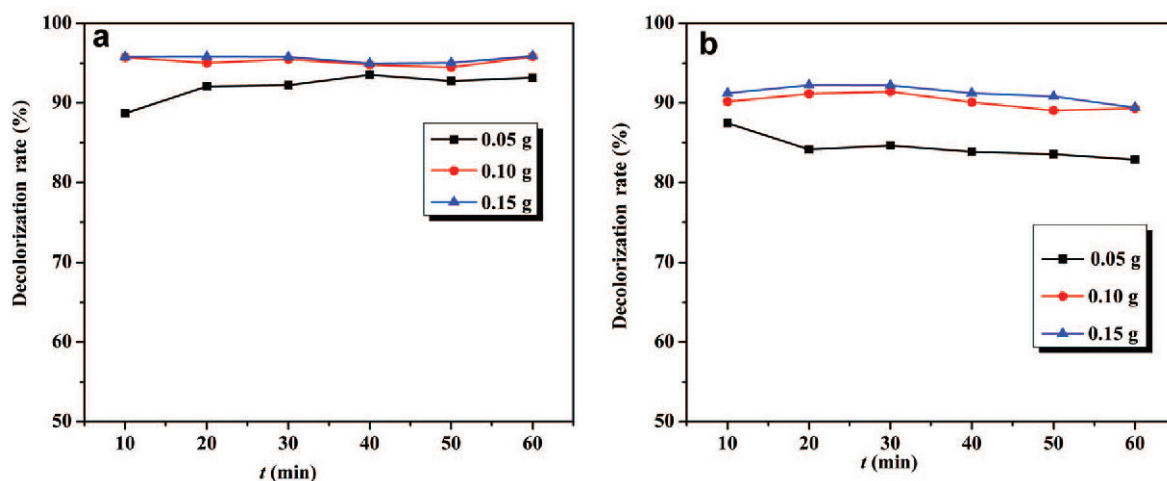


Figure 7. The effect of NaOH-modified fly ash (modified with 6 mol/L NaOH) on the decolorization rate of (a) MB and (b) AF. Experiment conditions: pH = 2, 30°C, 50 mL volume, and 30 mg/L initial MB or AF concentration.

Increases in the decolorization rate with increased amounts of adsorbent can be attributed to the greater adsorbent surface areas and more available adsorption sites, which led to enhanced dye removal efficiency.

Effect of solution pH on decolorization rate

Solution pH is an important factor that influences the degree of dye ionization and the adsorbent surface active sites. The effects of pH on MB or AF adsorption by NaOH-modified fly ash (modified with 6 mol/L NaOH) were studied to gain further insight into adsorption processes in the pH range of 2–10. When pH was <4, the decolorization rate of NaOH-modified fly ash increased significantly with increasing pH (Figure 8a). The highest MB adsorption was achieved at a pH of approximately 4. A slight decrease of decolorization rate was found at pHs of 4–8. The

decolorization rate significantly decreased when pH was increased from 8 to 12. Experimental measurements revealed a high rate of AF decolorization by NaOH-modified fly ash could be achieved at pH 2, which slightly decreased with an increase in pH (Figure 8b). Hence, the NaOH-modified fly ash was advantageous for AF adsorption under acidic conditions, while adsorption declined under alkaline and neutral conditions. Experimental measurements revealed, therefore, that the MB and AF adsorption capacity of NaOH-modified fly ash decreased under neutral and alkaline conditions because the surface properties of the NaOH-modified fly ash and form of the dye were changed by pH (Figure 8a, 8b). The dyes experience different physical and electrostatic forces due to differences in structure, molecular size, and functional groups. The modified fly ash environment is

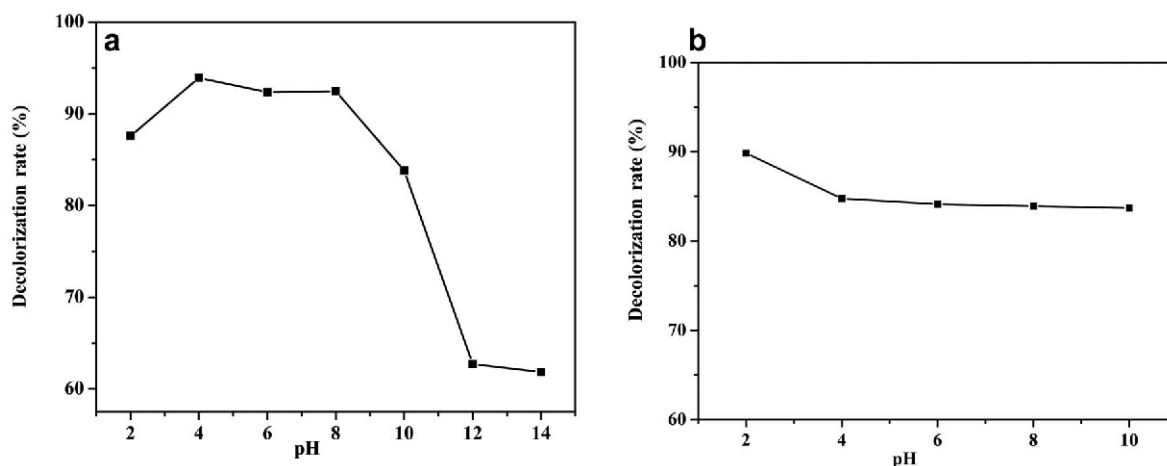


Figure 8. The effect of solution pH on (a) MB and (b) AF decolorization rate. Experiment conditions: 0.10 g of the NaOH-modified fly ash (modified with 6 mol/L NaOH), pH = 2, 30°C, 50 mL volume, and 30 mg/L initial MB or AF concentration.

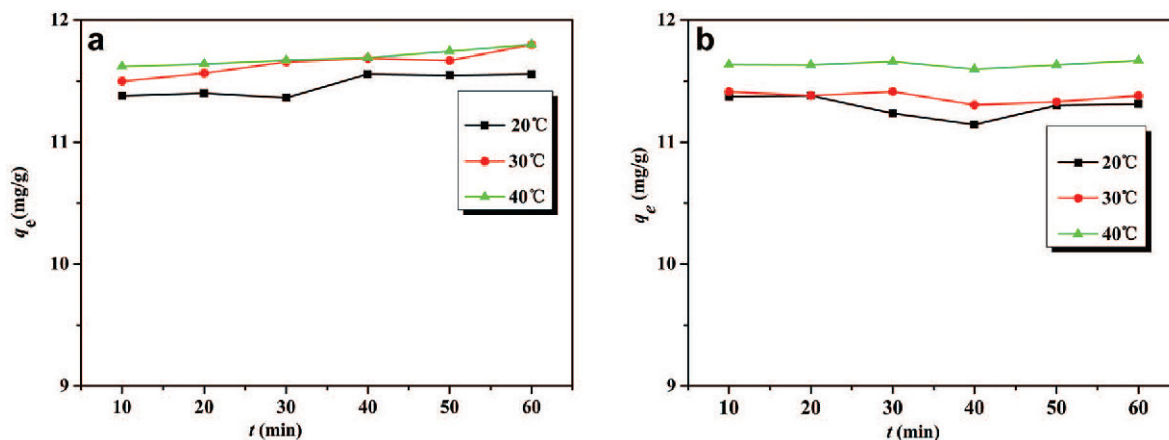


Figure 9. The effect of solution temperature on (a) MB and (b) AF decolorization rate. Experiment conditions: 0.10 g of NaOH-modified fly ash (modified with 6 mol/L NaOH), pH = 2, 50 mL volume, and 30 mg/L of initial MB or AF concentration.

alkaline. Under neutral or alkaline conditions, an increased pH leads to increased repulsion between dye molecules and modified fly ash surfaces.

Effect of solution temperature on decolorization rate

Experiments to determine the effects of solution temperature on dye decolorization were conducted. The equilibrium MB and AF adsorption capacity at different solution temperatures vs. contact time were measured (Figure 9). Increasing the temperature from 20 to 40°C produced no significant effect on decolorization (Figures 9a, 9b). The equilibrium adsorption capacity in 10 min of the NaOH-modified fly ash for MB and AF increased from 11.38 and 11.37 at 20°C to 11.62 and 11.64 mg/g at 40°C, respectively. The equilibrium adsorption capacity in 30 min of NaOH-modified fly ash for MB and AF were 11.36 and 11.23 mg/g at 20°C, 11.66 and 11.41 mg/g at 30°C, and 11.67 and 11.66 mg/g at 40°C, respectively. This indicates that the adsorption process of NaOH-modified fly ash for MB and AF was mainly physical adsorption.

Effect of initial solution concentration on decolorization rate

The effects of initial solution concentration on the adsorption capacity (q_t) of NaOH-modified fly ash samples were investigated at initial concentrations of 20–40 mg/L. Experimental measurements revealed almost complete removal of MB and AF by NaOH-modified fly ash after a sufficient contact time under the given experimental conditions, and the initial solution concentration affected the contact time required to reach adsorption equilibrium (Figure 10). Experimental measurements revealed that the adsorption capacity increased significantly with increased contact time and greater than 90% of MB and AF were removed during the first 10 min (Figure 10). As contact times were >10 min, the adsorption capacity remained almost constant, indicating that adsorption equilibrium of MB and AF on NaOH-modified fly ash was reached. The equilibrium adsorption capacities of NaOH-modified fly ash for MB and AF in 10 min increased from 17.67 and

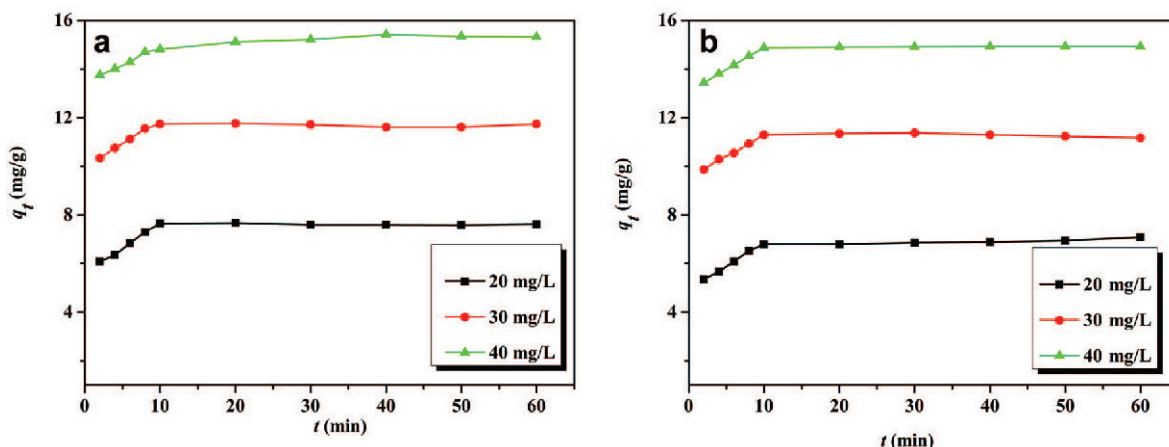


Figure 10. The effect of initial solution concentration on the decolorization rate of (a) MB and (b) AF. Experiment conditions: 0.10 g of NaOH-modified fly ash (modified with 6 mol/L NaOH), pH = 2, 50 mL solution volume, and 30°C.

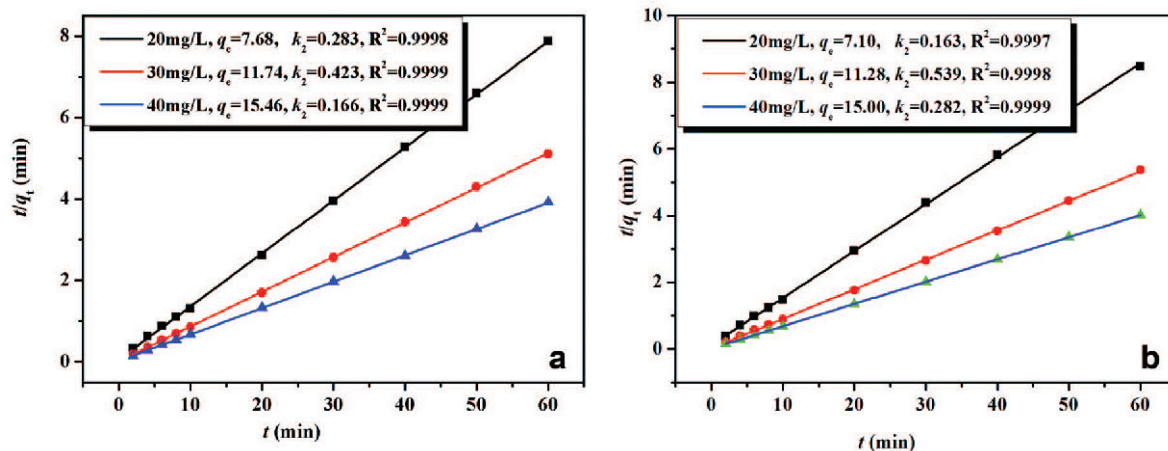


Figure 11. The pseudo-second order model for adsorption of (a) MB and (b) AF by NaOH-modified fly ash at different initial solution concentrations. The experimental conditions: 0.10 g of NaOH-modified fly ash (modified with 6 mol/L NaOH), pH = 2, 50 mL solution volume, and 30°C.

7.09 to 14.81 and 14.98 mg/g, respectively, when initial concentrations were increased from 20 to 40 mg/L.

Adsorption kinetics

The adsorption process and the amount adsorbed could be effectively predicted by the adsorption kinetics model. A simple kinetics model, such as a first-order rate equation, could not describe the adsorption process in the solid/liquid system. The surface physical and chemical properties of solid adsorbents are not the same, and adsorption includes two indivisible processes of mass transfer and adsorption. The pseudo-second order rate equation, however, revealed the behavior of the solid adsorbents and the whole adsorption process. The experimental data for MB and AF adsorption to NaOH-modified fly ash was, therefore, fitted using the pseudo-second model, expressed as follows (Ma *et al.*, 2015):

$$\frac{t}{q_t} = \frac{1}{k_2 q_e^2} + \left(\frac{1}{q_e} \right) t \quad (3)$$

where k_2 (g/mg·min) is the rate constant, which can be calculated from the intercept of a plot of t/q_t vs. t/q_e (Figure 11). Experimental measurements revealed that the correlation coefficients (R^2) of such plots reached 0.999, indicating that equation 3 gives reliable fits of the adsorption experimental data (Figure 11). Hence,

equation 3 was used to model the MB and AF adsorption processes to the NaOH-modified fly ash. The equilibrium adsorption values ($q_{e,cal}$) calculated using this expression were close to the experimental values ($q_{e,exp}$) and confirmed further that the process followed pseudo-second order reaction kinetics (Table 2).

Adsorption isotherms

To obtain the maximum adsorption capacity, adsorption isotherms were constructed using initial solution concentrations of 10–100 mg/L. The plot of equilibrium adsorption capacity (q_e) vs. equilibrium concentration (c_e) revealed an L-shape behavior based on the Giles' classification (Hameed *et al.*, 2008; Ge *et al.*, 2015) (Figure 12). The value of q_e increased dramatically as c_e increased in the range of lower dye concentrations (<30 mg/L) which indicates a high affinity between MB or AF and the NaOH-modified fly ash surfaces. As for higher dye concentrations (>50 mg/L), increasing c_e had no further effect on q_e , as revealed by the plateau in the c_e vs. q_e plot. In other words, the dye adsorption sites became saturated at the higher concentrations. To glean further information regarding the interactions between the dyes and the NaOH-modified fly ash, the data were re-plotted (Figure 12 insets) according to the linear forms of the Langmuir and Freundlich isotherms (equations 4 and 5,

Table 2. Kinetics parameters (mg/L) for dye adsorption on NaOH-modified fly ash (modified with 6 mol/L NaOH).

Pseudo-second model parameters	MB			AF		
	$c_0 = 20$	$c_0 = 30$	$c_0 = 40$	$c_0 = 20$	$c_0 = 30$	$c_0 = 40$
k_2 (g/mg·min)	0.283	0.423	0.166	0.163	0.539	0.282
$q_{e,cal}$ (mg/g)	7.68	11.74	15.46	7.10	11.28	15.00
R^2	0.9998	0.9999	0.9999	0.9997	0.9998	0.9999
$q_{e,exp}$ (mg/g)	7.63	11.71	15.07	7.20	11.44	14.96

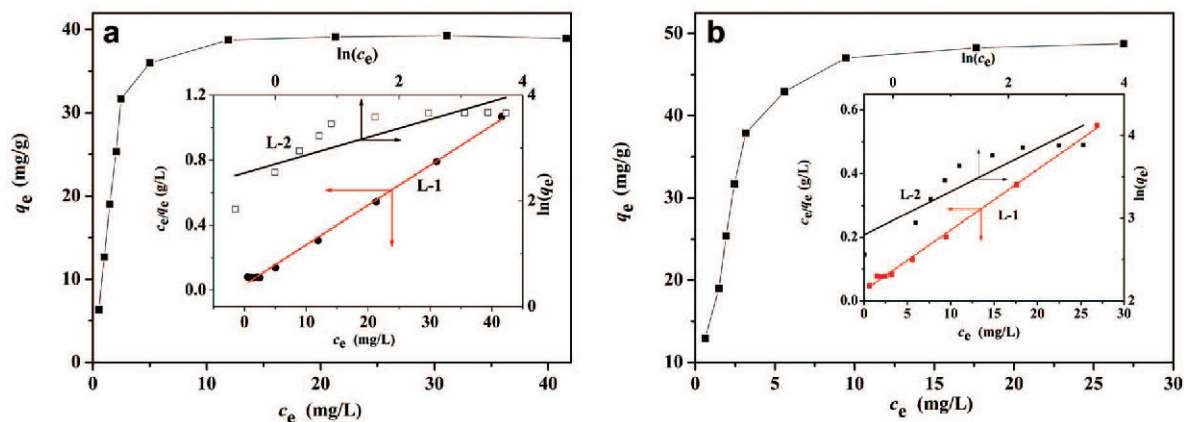


Figure 12. Adsorption isotherm of (a) MB and (b) AF on NaOH-modified fly ash. Inset contains data fitted to Langmuir (L-1) and Freundlich (L-2) models. Symbols indicate experimental data. Solid lines represent the fitted curves. The experimental conditions: 0.10 g of NaOH-modified fly ash (modified with 6 mol/L NaOH), pH = 2, 50 mL of solution, 30°C, and 10–100 mg/L initial MB or AF concentration.

respectively) (Langmuir, 1918; Freundlich, 1906; Huang *et al.*, 2015; Yin *et al.*, 2014):

$$\frac{c_e}{q_e} = \frac{c_e}{q_m} + \frac{1}{q_m K_L} \quad (4)$$

$$\ln q_e = \ln K_F + \frac{1}{n_F} \ln c_e \quad (5)$$

where q_m is the maximum adsorption capacity of the NaOH-modified fly ash for the dye (mg dye/g fly ash), K_L (L/mg) is the Langmuir adsorption constant, K_F is the Freundlich constant, and n_F is the constant that indicates adsorption intensity. Results clearly indicated that the data follow the Langmuir model more closely than the Freundlich model for both the MB and AF dyes (insets to Figures 12a and 12b, respectively), R^2 values of 0.9971 and 0.9965, respectively. Values for K_L and q_m , calculated from the intercept and slope of the c_e/q_e vs. c_e plots, respectively, were 0.687 L/mg and 40.98 mg/g for MB and 0.583 L/mg and 52.63 mg/g for AF. Assuming the original assumptions of the Langmuir equation hold for this liquid/solid system, the adsorption of MB or AF onto the NaOH-modified fly ash mainly occurred at specific sites with a homogeneous adsorption energy, all sites were equivalent, and no interactions occurred between the adsorbate molecules.

CONCLUSIONS

A novel low-cost modified fly ash was successfully prepared and used for the adsorption of dyes from aqueous solutions. Scanning electron microscopy, X-ray diffraction, and N_2 adsorption isotherm data showed that the NaOH-activated fly ash was characterized by macropores with a high BET surface area that was approximately twice as large as the pristine fly ash. The adsorption behavior of the activated fly ash was

evaluated by considering dye concentration, adsorbent weight, solution temperature, pH, and contact time. The adsorption kinetics were successfully modeled using a pseudo-second order rate equation and adsorption was successfully modeled using the Langmuir adsorption isotherm.

ACKNOWLEDGMENTS

This work was supported by the National Natural Science Foundation of China (Grant No. 21406188) and the Natural Science Foundation of the Department of Science & Technology of Shaanxi (Grant No. 2015KJXX-38).

REFERENCES

- Ahmed, Z.T., Hand, D.W., Watkins, M.K., and Sutter, L.L. (2014) Combined adsorption isotherms for measuring the adsorption capacity of fly ash in concrete. *ACS Sustainable Chemistry & Engineering*, **2**, 614–620.
- Akar, T., Celik, S., Ari, A.G., and Akar, S.T. (2013) Removal of Pb^{2+} ions from contaminated solutions by microbial composite: combined action of a soilborne fungus *Mucor plumbeus* and alunite matrix. *Chemical Engineering Journal*, **215–216**, 626–634.
- Akkaya, R. (2013) Removal of radioactive elements from aqueous solutions by adsorption onto polyacrylamide-expanded perlite: Equilibrium, kinetic, and thermodynamic study. *Desalination*, **321**, 3–8.
- Anirudhan, T.S., Rijith, S., and Suchithra, P.S. (2010) Preparation and characterization of iron(III) complex of an amino-functionalized polyacrylamide-grafted lignocelluloses and its application as adsorbent for chromium(VI) removal from aqueous media. *Journal of Applied Polymer Science*, **115**, 2069–2083.
- Baur, G.B., Yuranov, I., and Lioubov, K.M. (2015) Activated carbon fibers modified by metal oxide as effective structured adsorbents for acetaldehyde. *Catalysis Today*, **249**, 252–258.
- Cavka, J.H., Grande, C.A., Mondino, G., and Blom, R. (2014) High pressure adsorption of CO_2 and CH_4 on Zr-MOFs. *Industrial & Engineering Chemistry Research*, **53**, 15500–15507.
- Choi, S., Drese, J.H., and Jones, C.W. (2009) Adsorbent materials for carbon dioxide capture from large anthropo-

- genic point sources. *ChemSusChem*, **2**, 796–854.
- Freundlich, H.M.F. (1906) Over the adsorption in solution, *Journal of Physical Chemistry*, **57A**, 385–470.
- Frydrych, M., Wan, C.Y., Stengler, R., O’Kelly, K.U., and Chen, B.Q. (2011) Structure and mechanical properties of gelatin/sepiolite nanocomposite foams, *Journal of Materials Chemistry*, **21**, 9103–9111.
- Fu, F., Gao, Z.W., Gao, L.X., and Li, D.S. (2011) Effective adsorption of anionic dye, alizarin red S, from aqueous solutions on activated clay modified by iron oxide. *Industrial & Engineering Chemistry Research*, **50**, 9712–9717.
- Ge, X.Y., Tian, F., Wu, Z.L., Yan, Y.J., Cravotto, G., and Wu, Z.S. (2015) Adsorption of naphthalene from aqueous solution on coal-based activated carbon modified by microwave induction: Microwave power effects. *Chemical Engineering and Processing*, **91**, 67–77.
- Gupta, S.S. and Bhattacharyya, K.G. (2012) Adsorption of heavy metals on kaolinite and montmorillonite: A review. *Physical Chemistry Chemical Physics*, **14**, 6698–6723.
- Gupta, S.S. and Bhattacharyya, K.G. (2014) Adsorption of metal ions by clays and inorganic solids. *RSC Advances*, **4**, 28537–28586.
- Hameed, B.H., Tan, I.A.W., and Ahmad, A.L. (2008) Adsorption isotherm kinetic modeling and mechanism of 2,4,6-trichlorophenol on coconut husk-based activated carbon. *Chemical Engineering Journal*, **144**, 144235–144244.
- Hassan, M.M., Schiermeister, L., and Staiger, M.P. (2015) Thermal, chemical and morphological properties of carbon fibres derived from chemically pre-treated wool fibres. *RSC Advances*, **5**, 55353–55362.
- Huang, S.Y., Yan, B., Wang, S.P., and Ma, X.B. (2015) Recent advances in dialkyl carbonates synthesis and applications. *Chemical Society Reviews*, **44**, 3079–3116.
- Idris, N.M., Jayakumar, M.K.G., Bansal, A., and Zhang, Y. (2015) Up conversion nanoparticles as versatile light nanotransducers for photoactivation applications. *Chemical Society Reviews*, **44**, 1449–1478.
- Ji, Q.H., Tabassum, S., Yu, G.X., Chu, C.F., and Zhang, Z.J. (2015) A high efficiency biological system for treatment of coal gasification wastewater – a key in-depth technological research. *RSC Advances*, **5**, 40402–40413.
- Kim, H., Lee, B., and Byeon, S.H. (2015) The inner filter effect of Cr(VI) on Tb-doped layered rare earth hydroxylchlorides: new fluorescent adsorbents for the simple detection of Cr(VI). *Chemical Communications*, **51**, 725–728.
- Koukouzas, N., Vasilatos, C., Itskos, G., Mitsis, I., and Moutsatsou, A. (2010) Removal of heavy metals from wastewater using CFB-coal fly ash zeolitic materials. *Journal of Hazardous Material*, **173**, 581–588.
- Langmuir, I. (1918) The adsorption of gases on plane surfaces of glass, mica and platinum. *Journal of the American Chemical Society*, **40**, 1361–1403.
- Lee, J.D., Lee, S.H., Jo, M.H., Park, P.K., Lee, C.H., and Kwak, J.W. (2000) Effect of coagulation conditions on membrane filtration characteristics in coagulation-microfiltration process for water treatment. *Environmental Science & Technology*, **34**, 3780–3788.
- Lee, H., Kim, D., Kim, J., Ji, M.K., Han, Y.S., Park, Y.T., Yun, H.S., and Choi, J. (2015) As(III) and As(V) removal from the aqueous phase via adsorption onto acid mine drainage sludge (AMDS) alginate beads and goethite alginate beads. *Journal of Hazardous Material*, **292**, 146–154.
- Liao, M.S., Zhao, Y.H., Ning, P.G., Cao, H.B., Wen, H., and Zhang, Y. (2014) Optimal design of solvent blend and its application in coking wastewater treatment process. *Industrial & Engineering Chemistry Research*, **53**, 15071–15079.
- Liu, J., Thallapally, P.K., McGrail, B.P., Brown, D.R., and Liu, J. (2012) Progress in adsorption-based CO₂ capture by metal-organic frameworks. *Chemical Society Reviews*, **41**, 2308–2322.
- Liu, D.Q., Zheng, Z.Z., Wang, C.Q., Yin, Y.Q., Liu, S.Q., Yang, B., and Jiang, Z.H. (2013) CdTe quantum dots encapsulated ZnO nanorods for highly efficient photoelectrochemical degradation of phenols. *Journal of Physical Chemistry C*, **117**, 26529–26537.
- Ma, J., Zhuang, Y., and Yu, F. (2015) Facile method for the synthesis of a magnetic CNTs-C@Fe-chitosan composite and its application in tetracycline removal from aqueous solutions. *Physical Chemistry Chemical Physics*, **17**, 15936–15944.
- Petit, C. and Bandosz, T.J. (2011) Synthesis, characterization, and ammonia adsorption properties of mesoporous metal-organic framework (MIL(Fe))–graphite oxide composites: Exploring the limits of materials fabrication. *Advanced Functional Materials*, **21**, 2108–2117.
- Pizarro, J., Castillo, X., Jara, S., Ortiz, C., Navarro, P., Cid, H., Rioseco, H., Barros, D., and Belzile, N. (2015) Adsorption of Cu²⁺ on coal fly ash modified with functionalized mesoporous silica. *Fuel*, **156**, 96–102.
- Sevilla, M. and Mokaya, R. (2014) Energy storage applications of activated carbons: supercapacitors and hydrogen storage. *Energy & Environmental Science*, **7**, 1250–1280.
- Shi, Z.L., Yao S.H., and Sui, C.C. (2011) Application of fly ash supported titanium dioxide for phenol photodegradation in aqueous solution. *Catalysis Science & Technology*, **1**, 817–822.
- Sing, K.S.W., Everett, D.H., Haul, R.A.W., Mouscou, L., Pierotti, R.A., Rouquerol, J., and Siemieniowska, T. (1985) Reporting physisorption data for gas/solid systems with special reference to the determination of surface area and porosity. *Pure and Applied Chemistry*, **57**, 603–619.
- Sun, Y.B., Chen, C.L., Tan, X.L., Shao, D.D., Li, J.X., Zhao, G.X., Yang, S.B., Wang, Q., and Wang, X.K. (2012) Enhanced adsorption of Eu(III) on mesoporous Al₂O₃/expanded graphite composites investigated by macroscopic and microscopic techniques. *Dalton Transactions*, **41**, 13388–13394.
- Tang, S.C.N., Yan, D.Y.S.I., and Lo, M.C. (2014) Sustainable wastewater treatment using micro-sized magnetic hydrogel with magnetic separation technology. *Industrial & Engineering Chemistry Research*, **53**, 15718–15724.
- Torrellas, S.A., Lovera, R.G., Escalona, N., Sepúlveda, C., Sotelo, J.L., and Garcí̃a, J. (2015) Chemical-activated carbons from peach stones for the adsorption of emerging contaminants in aqueous solutions. *Chemical Engineering Science*, **279**, 788–798.
- Upadhyay, R., Soin, K.N., and Roy, S.S. (2014) Role of graphene/metal oxide composites as photocatalysts, adsorbents and disinfectants in water treatment: A review. *RSC Advances*, **4**, 3823–3851.
- Wang, M.S., Liao, L.B., Zhang, X.L., Li, Z.H., Xia, Z.G., and Cao, W.D. (2011) Adsorption of low-concentration ammonium onto vermiculite from Heibei Province, China. *Clays and Clay Minerals*, **59**, 459–465.
- Wang, Y.Z., Wang, W.B., and Wang, A.Q. (2013) Efficient adsorption of methylene blue on an alginate-based nanocomposite hydrogel enhanced by organo-illite/smectite clay. *Chemical Engineering Journal*, **228**, 132–139.
- Wang, X.M., Chen, L.M., Liu, Y.N., and Huang, J.H. (2014a) Macroporous crosslinked polydivinylbenzene/polyacryli-diethylenetriamine (PDVB/PADETA) interpenetrating polymer networks (IPNs) and their efficient adsorption to o-aminobenzoic acid from aqueous solution. *Journal of Colloid and Interface Science*, **429**, 83–87.

- Wang, J.Z., Zhao, G.H., Li, Y.F., Zhu, H., Peng, X.M., and Gao, X. (2014b) One-step fabrication of functionalized magnetic adsorbents with large surface area and their adsorption for dye and heavy metal ions. *Dalton Transactions*, **43**, 11637–11645.
- Yang, S.X., Wang, L.Y., Zhang, X.D., Yang, W.J., and Song, G.L. (2015) Enhanced adsorption of Congo red dye by functionalized carbon nanotube/mixed metal oxides nanocomposites derived from layered double hydroxide precursor. *Chemical Engineering Journal*, **275**, 315–321.
- Yin, C.Y., Ng, M.F., Saunders, M., Goh, B.M., Senanayake, G., Sherwood, A., and Hampton, M. (2014) New insights into the adsorption of aurocyanide ion on activated carbon surface: Electron microscopy analysis and computational studies using fullerene-like models. *Langmuir*, **30**, 7703–7709.
- Zhao, D.H., Zhang, Y.L., Wei, Y.P., and Gao, H.W. (2009) Facile eco-friendly treatment of a dye wastewater mixture by *in situ* hybridization with growing calcium carbonate. *Journal of Material Chemistry*, **19**, 7239–7244.
- Zhang, C.L., Wu, L., Cai, D.Q., Zhang, C.Y., Wang, N., Zhang, J., and Wu, Z.Y. (2013a) Adsorption of polycyclic aromatic hydrocarbons (fluoranthene and anthracenemethanol) by functional graphene oxide and removal by pH and temperature-sensitive coagulation. *ACS Applied Materials & Interfaces*, **5**, 4783–4790.
- Zhang, J.X., Zhou, Q.X., and Li, W. (2013b) Adsorption of enrofloxacin from aqueous solution by bentonite. *Clay Minerals*, **48**, 627–637.
- Zheng, X.N., Wu, D.B., Su, T., Bao, S., Liao, C.A., and Wang, Q.G. (2014) Magnetic nanocomposite hydrogel prepared by ZnO-initiated photopolymerization for La(III) adsorption. *ACS Applied Materials & Interfaces*, **6**, 19840–19849.

(Received 9 November 2015; revised 13 June 2016; Ms. 1065; AE: A. Neumann)